# Heat-Transfer Model for Toroidal Transformers

Sujit Purushothaman, *Student Member, IEEE*, and Francisco de León, *Senior Member, IEEE*

***Abstract*—Toroidal transformers provide increased design flexibility, efficiency, and compact design when compared to traditional shell- or core-type transformers. In this paper, the steady-state thermal analysis for toroidal transformers is conducted using a lumped parameter model which can be applied to small power and distribution-grade toroidal transformers as well. Two cases are considered: 1) when the transformer is kept in open air and 2) when it is installed in sealed enclosures. The detailed model includes the effects of the number of turns of windings, number of layers, insulation properties, and geometric properties of the transformer. The model is capable of finding the hotspots that are of paramount importance for the designer. The model parameters are calculated from the design (geometrical) information; therefore, it is suitable to be included in the design loop of transformer design software. The results are compared with finite-element simulations and lab tests on prototypes of various power ratings fitted with thermocouples to record internal temperatures. The model can also be used with varied external media and encapsulation, such as air, oil, and epoxy.**

***Index Terms*—Equivalent thermal circuit, finite-element method, heat transfer, thermal rating, toroidal transformers.**

## NOMENCLATURE

| | |
|---|---|
| HV | High voltage. |
| LV | Low voltage. |
| HST | Hottest spot temperature. |
| $Q_{\text{loss}}$ | Total ohmic loss in transformer (in watts). |
| $h$ | Heat-transfer coefficient $[\text{W}/\text{m}^2.\text{K}]$ . |
| $k$ | Thermal conductivity (in W/m.K) |
| $Nu$ | Nusslet number. |
| $Gr$ | Grashoff's number. |
| $Pr$ | Prandtl number. |
| $Ra$ | Rayleigh number. |

## I. INTRODUCTION

THE first transformer was built by Faraday in 1831 on a toroidal core [1]. These days, toroidal transformers are mostly being used in power supplies for avionics, audio systems, and electronic equipment rated for low voltages and relatively low power [2], [3]. Transformers used in bulk power transmission are of core-type or shell-type construction. Over the years, considerable research has been conducted on thermal modeling of oil-immersed transformers. Equivalent electrical circuits with nonlinear resistors have been used to model the air or oil convection currents [4] in transformers. Models based on the equivalent thermal circuit have also been proposed to determine the top-oil temperature (TOT) and the hottest spot temperature (HST) [5]–[7]. A finite-element method (FEM)-based 3-D model was used to simulate and study the temperature distribution within a toroidal transformer [8]. The application of toroidal transformers in power transmission and distribution at medium voltage (MV) is stunted. This so not only because its construction could be more expensive than traditional designs, but perhaps due to the lack of previously published research work.

The toroidal construction has many advantages over standard power transformers. For example: the lack of an air gap in the toroidal core allows for higher design flux density. The closed geometry (where the second winding completely covers the first) produces a transformer with a smaller leakage inductance than that of traditional designs producing transformers with small regulation. In addition, the acoustic noise and electromagnetic emissions are smaller. In an effort to forward the advantages of toroidal transformers to distribution systems, the U.S. Department of Energy has funded a project to design and develop toroidal transformers for MV distribution systems. This paper is part of a series of papers describing solutions to problems related to the design and construction of these utility-grade transformers. Equations to accurately compute the leakage impedance have been obtained and verified experimentally in [9]. The insulation design based on the propagation of the impulse wave in windings on the toroidal core has been presented in [10].

The power rating of a transformer is limited by the temperature of the hot spots. This paper describes a procedure to set up a thermal model of toroidal transformers. The model can accurately predict the temperature of each winding layer along four directions. This model can be used to study temperature distribution for transformers used in MV distribution systems.

Results from the model are compared with finite-element simulations yielding a good match. The proposed model was also validated with a set of prototypes (of various power ratings) especially built with thermocouples placed at strategic locations within the transformer. The model has proven to be sufficiently accurate and efficient for practical implementation in a design program.

## II. GEOMETRIC ARRANGEMENT

Traditional core-type or shell-type transformers consist of uniform windings around the core. This makes it easy to perform thermal studies using lumped parameter thermal circuits

Manuscript received May 11, 2011; revised December 12, 2011; accepted January 22, 2012. Date of publication March 06, 2012; date of current version March 28, 2012. This work was supported in part by the U.S. Department of Energy under Grant DEOE0000072. Paper no. TPWRD-00390-2011.

The authors are with the Polytechnic Institute of New York University, Brooklyn, NY 11201 USA (e-mail: sujitp@ieee.org; fdeleon@poly.edu).

Color versions of one or more of the figures in this paper are available online at http://ieeexplore.ieee.org.

Digital Object Identifier 10.1109/TPWRD.2012.2185956

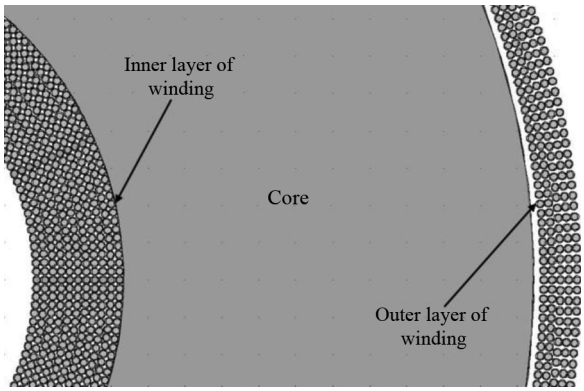


Fig. 1. Top view of the toroidal transformer showing winding distribution.

[4]–[7]. Fig. 1 shows the uneven winding distribution due to the geometry of the toroidal core. The core has an unequal surface area on the inside and the outside surface because of the smaller radius (Perimeter $= 2\pi\ r$). Hence, the conductor spacing is more on the outside than on the inside. Since the cross-sectional area of the conductor remains the same everywhere, the conductors' bundle is thicker on the inside and thinner on the outside. This is also applicable to any insulation wrapped between layers. Since a large temperature gradient exists within an insulator, this nonuniform distribution of insulation thickness on the inside and outside is of critical importance to this study.

The unequal surface areas and the nonuniform distribution of windings on the toroidal core leads to a complex analysis explained in Section IV.

The transformer under study consists of a toriodal core, covered by a layer of insulation. The LV windings with $n$ layers are wound first on the insulated core followed by the $m$ layers of the HV windings. The insulation class requirements may cause insulation layers to be added between layers of the HV windings. This reduces thermal performance and, hence, accurate thermal modeling is a crucial step in the design of a distribution-grade toroidal transformer.

## III. Equivalent Thermal Circuit

The thermal-electric analogy for the analysis of heat-transfer phenomena is well known and a good explanation can be found in [14] and [16]. The core and both windings are metallic materials (steel and copper) and, hence, offer high thermal conductivity $k$. The windings carry current and produce heat due to ohmic losses. The eddy current losses and hysteresis losses constitute the core losses. Therefore, in the electrical equivalent circuit, the windings and the core are modeled as current sources. The insulation is essentially made of several layers of thin Mylar wound tape, having low electrical and thermal conductivity and, so, the insulation layers are modeled as thermal resistors in the circuit.

Fig. 2 shows the thermal equivalent circuit superimposed on the axial slice geometry of a typical toroidal transformer. The uneven distribution of windings causes an uneven temperature field around the core. Therefore, an equivalent thermal circuit is proposed for each of the four directions; namely, top, outer, bottom, and inner directions. The detailed equivalent thermal circuit in the outer direction for the toroidal transformer is as

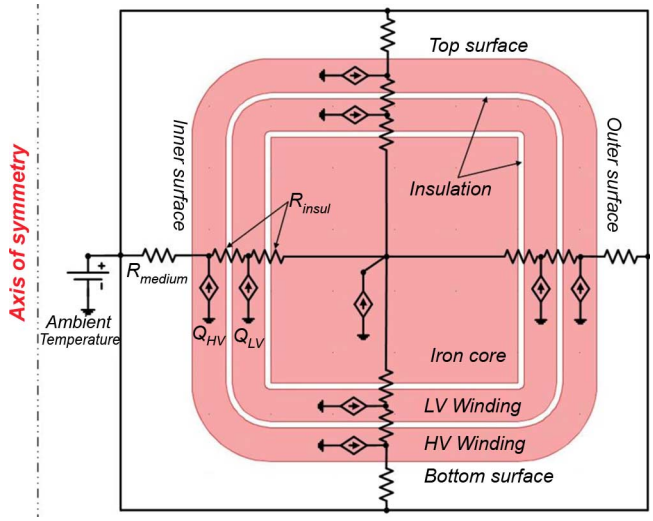


Fig. 2. The 2-D axial symmetric geometry of the toroidal transformer.

shown in Fig. 3. The effect of insulation between core laminations is considered by adding resistances in the inner and outer directions at the core node. The circuits for the other three directions are similar with different parameter values. All circuits are connected at the core (center), producing a cross-shaped equivalent circuit.

The heat flow in the inner and outer regions is a cylindrical thermal problem whereas that in the top and bottom regions is Cartesian.

The resistance of the top and bottom insulation layers can be computed as [14]

$$R_{\text{insul}} = \frac{t}{k\,A} \tag{1}$$

where $t$ is the thickness and $A$ is the surface area of the insulation layer. The resistance of the inner and outer insulation (cylindrical) layers can be computed as

$$R_{\text{insul}} = \frac{1}{2\pi\ k\ H_{\text{insul}}} \ln\left(\frac{\text{OD}}{\text{ID}}\right) \tag{2}$$

where OD and ID are the outer and inner diameters of the insulation layer, respectively. $H_{\text{insul}}$ is the height of the layer.

The heat loss in the $n$th layer $Ql_n$ is equal to total heat loss in the winding $Q$ times the ratio of the number of turns in the present layer $Nl_n$ to the total number of turns in the winding $N$

$$Ql_n = Q\frac{Nl_n}{N}. \tag{3}$$

Assuming the heat dissipated in the conductor per-unit length to be constant, $Ql_n$ times the ratio of a fraction of the length of a turn $l_x$ in the respective direction $x$ to the length of a turn in the $n$th layer $L_n$ gives the current sources in each directional circuit

$$(Ql_n)_x = Ql_n\frac{l_x}{L_n}. \tag{4}$$

The temperature of the surrounding medium is modeled as an ideal voltage source since it is assumed that the ambient temperature would not be affected by the presence of the transformer under consideration. The thermal resistance of the surrounding

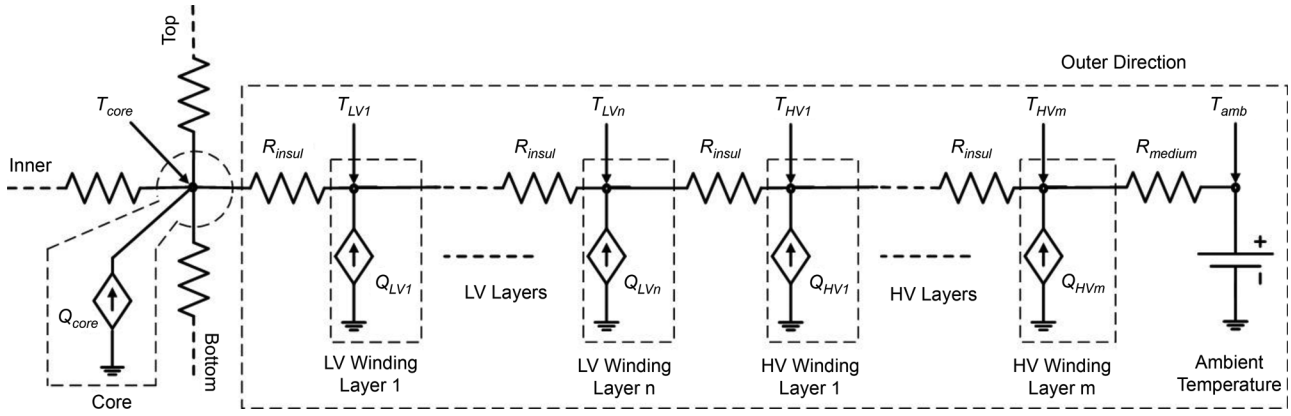


Fig. 3. The 2-D detailed thermal circuit in the outer direction for the toroidal transformer.

medium is highly dependent on the physical state of the medium (solid (epoxy), liquid (oil), or gas (air)). This resistance can be nonlinear and its computation is complex as described in the following section.

Since the model deals with steady-state calculations only, no capacitances are needed in the thermal equivalent circuit. The algorithm for computing the results is given in Appendix B.

## IV. Thermal Resistance of the Surrounding Medium

Fluid medium (air, oil) dissipate heat by convection and radiation. Convection is the phenomenon of heat transfer by conduction in moving media. Radiation is medium independent and accounts for 20%–30% of the total heat flux and, hence, should not be neglected.

This section explains the computation of the heat-transfer coefficient $h_{\rm conv}$ for natural convection in the laminar regime. $h_{\rm conv}$ is a function of the geometric arrangement, temperature, and properties of the convective medium of the surface under consideration. $h_{\rm conv}$ is given by [14] and [15]

$$h_{\rm conv} = \frac{Nu\, k}{L} \tag{5}$$

where $k$ is the thermal conductivity of the surrounding medium, $L$ is the characteristic length, and $Nu$ is the Nusselt number. In general, the relationship between $Nu$ and the Rayleigh number $Ra_L$ is given by (6) and depends on the orientation of the surface under consideration [13]

$$Nu = CRa_L^m. \tag{6}$$

For the top surface [13]

$$\begin{aligned} 10^4 \le Ra_L < 10^7; \quad C = 0.54; \quad m = 0.25 \\ 10^7 \le Ra_L < 10^9; \quad C = 0.15; \quad m = 0.334 \end{aligned} \tag{7}$$

and $L$ is the ratio of surface area to perimeter. For bottom surface, $C = 0.27$, $m = 0.25$, and $L$ is the length. For vertical faces, $L$ is the length and

$$Nu = 0.671 \times \left( \frac{Pr \times Ra_L}{Pr + 0.492 + (0.986 \times \sqrt{Pr})} \right)^{0.25}. \tag{8}$$

The expression for $Ra_L$ is given as follows [14], [15]:

$$Ra_L = Gr_L \times Pr \tag{9}$$

where $Gr_L$ is the Grashoff's number and $Pr$ is the Prandtl number, given by

$$Gr_L = \frac{g\beta(T_s - T_\infty)L^3}{\nu^2} \tag{10}$$

$$Pr = \frac{C_p \mu}{k} \tag{11}$$

$g$ acceleration due to gravity;

$\beta$ volumetric thermal expansion coefficient;

$\nu$ kinematic viscosity;

$C_p$ specific heat capacity at constant pressure;

$\mu$ dynamic viscosity.

The convective thermal resistance $R_{\rm conv}$ is given by

$$R_{\rm conv} = \frac{1}{h_{\rm conv}\, A}. \tag{12}$$

The radiative heat-transfer coefficient $h_{\rm rad}$ is calculated as [14], [15]

$$h_{\rm rad} = \varepsilon\sigma(T_s + T_\infty)(T_s^2 + T_\infty^2) \tag{13}$$

where $\varepsilon$ is the emissivity of the surface with area $A$, dissipating radiative heat flux; $T_s$ and $T_\infty$ are the surface temperature and temperature of the ambient surroundings, respectively; and $\sigma$ is the Stefan-Boltzmann's constant.

The radiative thermal resistance $R_{\rm rad}$ is given by

$$R_{\rm rad} = \frac{1}{h_{\rm rad}\, A}. \tag{14}$$

Since convection and radiation occur simultaneously at the surface, the total thermal resistance of the medium is the parallel combination of $R_{\rm conv}$ and $R_{\rm rad}$.

In the case of encapsulation of the transformer, the material (epoxy resin) may be treated as a solid insulation medium.

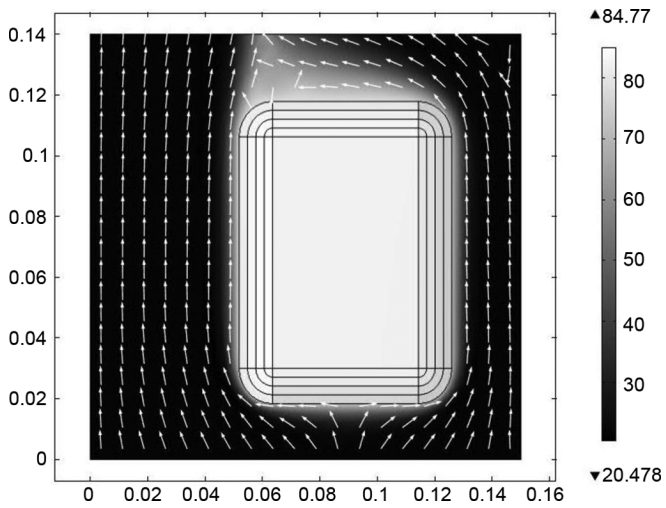


Fig. 4. FEM model of the toroidal transformer under test.

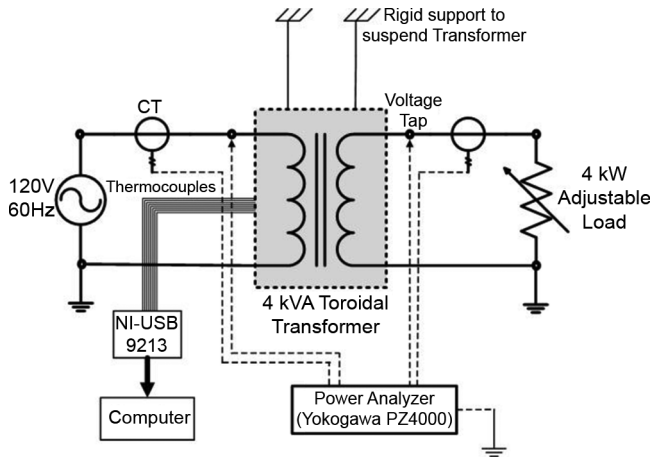


Fig. 5. Schematic for lab tests performed on the prototypes.

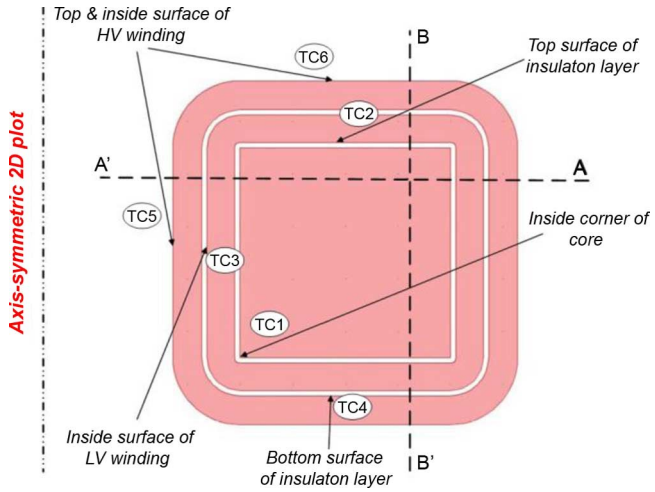


Fig. 6. Placement of thermocouples inside the prototype.

Hence, $R_{\text{conv}}$ would be substituted by (1) and (2) since now the heat transfer is done by conduction.

## V. Finite-Element Model

A 2-D axisymmetric model of the prototype was built in COMSOL Multiphysics [12] simulating open-air conditions. The model shown in Fig. 4 simulates a toroidal transformer suspended in air to ensure all surfaces contribute to heat dissipation.

The following set of nonlinear equations is solved simultaneously with the finite-elements method (FEM): The Navier–Stokes equation [14]

$$\rho\frac{\partial u}{\partial t}+\rho(u\cdot\nabla)u=-\nabla p+\mu\nabla^2u+\rho g \tag{15}$$

the continuity equation

$$\frac{\partial \rho}{\partial t}+\nabla\cdot(\rho u)=0 \tag{16}$$

and the energy equation

$$\rho C_p\frac{\partial T}{\partial t}+\rho C_p u\cdot\nabla T=\nabla\cdot(k\nabla T)+Q. \tag{17}$$

$T$ is temperature at a point, $\rho$ is the density, $p$ is the pressure, and $Q$ is the heat generated. $u$ is the velocity field which exists only for fluid (air or oil) domains and is zero for solid domains.

Fig. 4 shows the FEM surface plot for temperature $T$ along with an arrow plot showing fluid velocity $u$. The lower boundary of the model is fixed at 1 atm pressure $(p)$ and temperature $(T)$ at 22 °C. The pressure at the top boundary is also fixed at 1 atm pressure. It is also defined as a heat sink. The vertical surface is defined as heat insulation (zero temperature gradient). The vertical surface and transformer surfaces are defined as no-slip $(u=0)$. Internal boundaries representing interlayer insulation are defined as thermal resistive boundaries with the thickness calculated as described in Section II.

It must be noted that the solution of this highly nonlinear problem of natural convection is time consuming even in the most powerful PC computers [dual Intel Xeon processors running at 3.33 GHz with 96-GB random-access memory (RAM)] available today (2011). The FEM model has 4099 second degree elements and can take a couple of hours for a solution. This solution cannot be included in a design program which may take several iterations to obtain the final design. Hence, the need for a simple and accurate model is required which can yield the temperature distribution within the transformer without being computationally intensive.

## VI. Laboratory Tests

Laboratory tests were conducted on toroidal core prototypes of various power ratings to verify the proposed model. Fig. 5 presents the test schematic. The prototype (detailed in Appendix A) was suspended in air to simulate the conditions as given in Section V. A Yokogawa PZ-4000 power analyzer was used to measure input and output power of the prototype. A National Instruments NI-USB 9213 thermocouple measurement unit was used to record temperatures on a computer. The prototype has six thermocouples placed at locations internal to the transformer per Fig. 6. Cross-sections AA' and BB' depicted

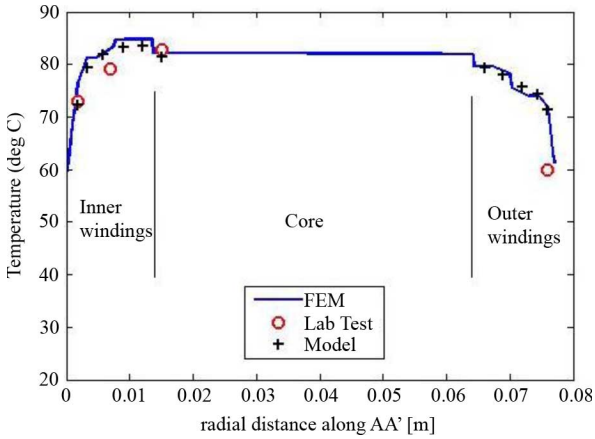


Fig. 7. Comparison of temperature distribution along section AA.

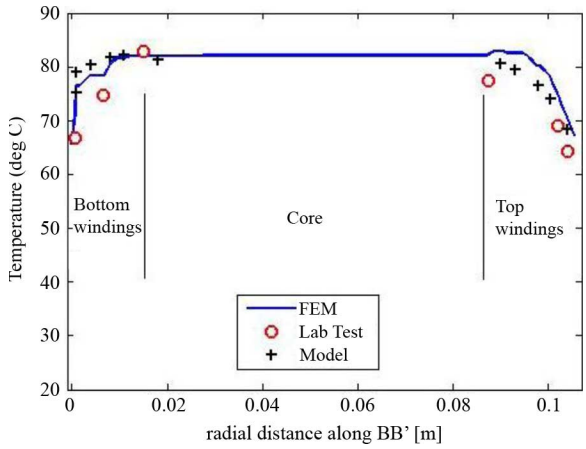


Fig. 8. Comparison of temperature distribution along section BB'.

in this figure are used later in Section VII to compare results. The transformer was fed from a constant voltage source while the load power was kept constant. The input power, output power, and the temperatures were recorded at intervals of 30 min until steady state was achieved per IEEE C57 [12]: the temperature does not change more than 2 °C in three hours. The difference in input and output power is the power dissipated in the transformer and is responsible for the temperature rise.

The estimation of power loss in individual windings and layers accurately is essential for this model. The mean length per turn times the total number of turns per layer would yield total resistance per layer. From this, the $I^2R$ loss can be calculated precisely.

## VII. Model Results

This section summarizes the results from the equivalent circuit, the finite-element simulations, and the lab test on the prototype. As shown in Fig. 6, horizontal cross section AA' is defined as a line starting from the inner surface to the external surface. Section AA' is used to plot temperatures in the inner windings, core, and outer windings. Fig. 7 presents this comparison. Similarly, cross-section BB' is defined from the bottom to the upper surface and is used to plot for bottom windings, core, and top windings. Fig. 8 presents the results along this section.

TABLE I
Result Comparison for Various Prototypes and Configurations.

| HST for Free Air Tests | | | | |
|---|---|---|---|---|
| Rating | Load | Max Temp.(Test)* | HST (Model) | HST (FEM) |
| 1 kVA | 1 kW | 83.9 | 85.5 | 85.5 |
| 2 kVA | 2 kW | 78.5 | 79.6 | 80.4 |
| 4 kVA | 4 kW | 82.8 | 84.3 | 84.7 |
| **HST for potted Transformer Tests** | | | | |
| 1 kVA | 1 kW | 86.4 | 89.0 | 88.8 |
| 4 kVA | 3.7 kW | 78.5 | 81.4 | 80.2 |
| **HST for Transformer in Enclosure Tests** | | | | |
| 2 kVA | 1.25 kW | 81.7 $T_{tank}$ = 43 | 79.0 $T_{tank}$ = 46.2 | 80.4 $T_{tank}$ = 45.4 |
| 4 kVA | 3 kW | 89.1 $T_{tank}$ = 48.9 | 87.0 $T_{tank}$ = 44.8 | 86.9 $T_{tank}$ = 43.9 |

* Unable to acquire the HST.

It is observed that the equivalent circuit behaves relatively accurately with the FEM model for the inner, outer, and bottom windings. The differences in the outer winding are larger. The prototype test results are also within practical error limits of the model (maximum differences of 4%). The HST in this transformer is located at the inner LV winding. The probe in the prototype was not exactly placed at the location of the hot spot and, therefore, was unable to catch the HST. In Table I, we report the maximum temperature measured, which is very close to the HST.

## VIII. Transformer in the Enclosure

Distribution-grade transformers are required to be enclosed in an airtight metallic enclosure for safety reasons. The enclosure may be solid (epoxy), liquid (oil), or air filled. The tank provides additional, although small, thermal resistance to the heat flux and, hence, raises the operating temperature of the transformer. The tank can be modeled as a single lumped resistance in series with the ambient temperature "voltage" source (Fig. 2), effectively raising the ambient temperature to $T_{\rm tank}$ given by

$$T_{\rm tank} = T_\infty + Q_{loss} \times R_{\rm tank} \tag{18}$$

where $T_{\rm tank}$ is the enclosure temperature and $R_{\rm tank}$ is the effective tank resistance.

The effective tank resistance $R_{\rm tank}$ can be calculated as

$$\frac{1}{R_{\rm tank}} = \frac{1}{R_{\rm top}} + \frac{1}{R_{\rm vertical}} + \frac{1}{R_{\rm bottom}} \tag{19}$$

where $R_{\rm top}$, $R_{\rm bottom}$, and $R_{\rm vertical}$ are the thermal resistances of the top, bottom, and vertical surfaces of the tank to the external medium. They can be evaluated from (6)–(8).

All equations presented in Section IV are applicable for the computation of temperature distribution within the transformer kept in an enclosure with the exception of the ambient temperature. This must equate to the temperature of enclosure $T_{\rm tank}$ since the transformer is not exposed to the surroundings at ambient temperature.

The algorithm to compute $T_{\rm tank}$ is presented in Appendix C.

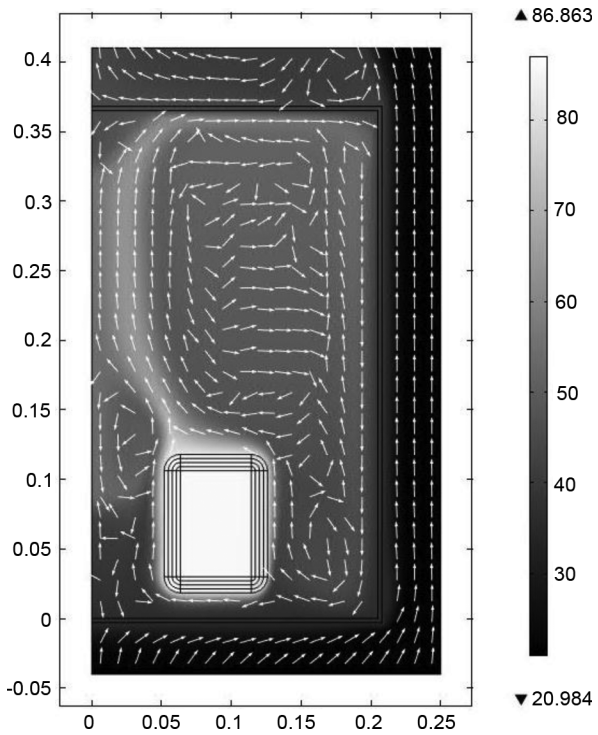


Fig. 9. FEM model of the toroidal transformer enclosed in a sealed enclosure under test.

### A. Laboratory Tests

Various laboratory tests were conducted on prototypes (used in earlier sections) kept in sealed enclosures, to study the derating effect that the tank would have on the transformer. A dry-type arrangement (air inside enclosure) was used for this setup. To avoid exceeding the temperature limitations of the prototypes, 75% rated load was used for these tests. The same procedure, as explained in Section VI, was followed for these tests.

### B. Finite-Element Simulations

FEM simulation with the enclosure modeled was used to compare results between the proposed model and the laboratory tests. Fig. 9 shows the FEM surface plot for temperature and an arrow plot for fluid velocity. The boundaries of the enclosure are closed since the fluid medium inside the enclosure is not allowed to escape. The equations solved and external boundary conditions are the same as explained in Section V.

### C. Results

Results comparing the steady-state temperature between the tests, FEM model, and proposed model are given in Figs. 10 and 11. The results are plotted along section AA' for the horizontal and BB' for the vertical temperature distribution within the transformer.

It is observed that the model predicts the temperature variation very well. The HST occurs at the same location (inner LV winding) as the transformer exposed to ambient. The maximum error is less than 4% and is observed around the HST.

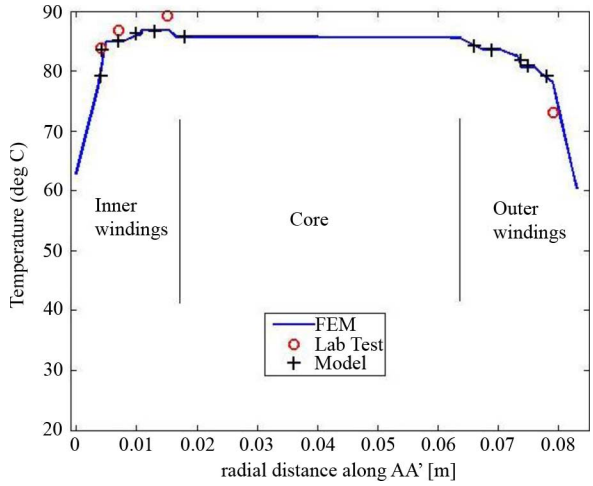


Fig. 10. Comparison of the temperature distribution along section AA' for transformer in a sealed enclosure.

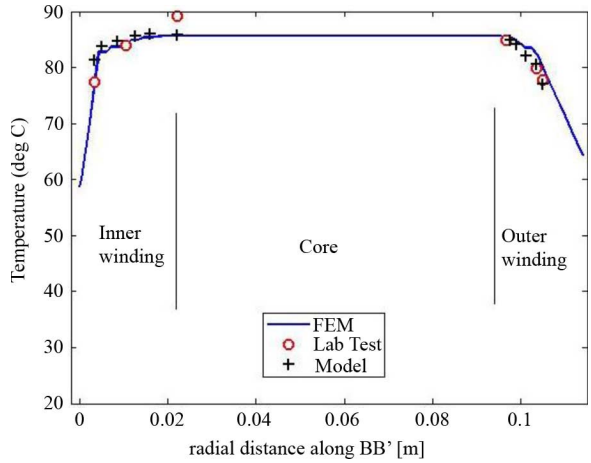


Fig. 11. Comparison of the temperature distribution along section BB' for transformer in a sealed enclosure.

## IX. Consolidated Results

A concise report of all tests conducted on the prototypes is presented in Table I. Five prototypes (3 standard and 2 encapsulated in epoxy) of various power ratings with thermocouples installed as described in Fig. 6 were tested until steady state was achieved per IEEE C57 [12]. The load column gives the constant electrical load connected at the transformer terminals. It is observed that encapsulation or enclosing the transformer leads to a derating. The comparisons of the HST from the tests, model, and FEM are provided. It must be noted that all of the results are within practical engineering error limits (less than 4%).

## X. Conclusion

This paper has presented a model that provides detailed insight into the variation of temperature within a toroidal transformer. The equivalent electrical circuit accurately models the nonlinear effects of convection and radiation and takes substantially less computational effort when compared to FEM. The

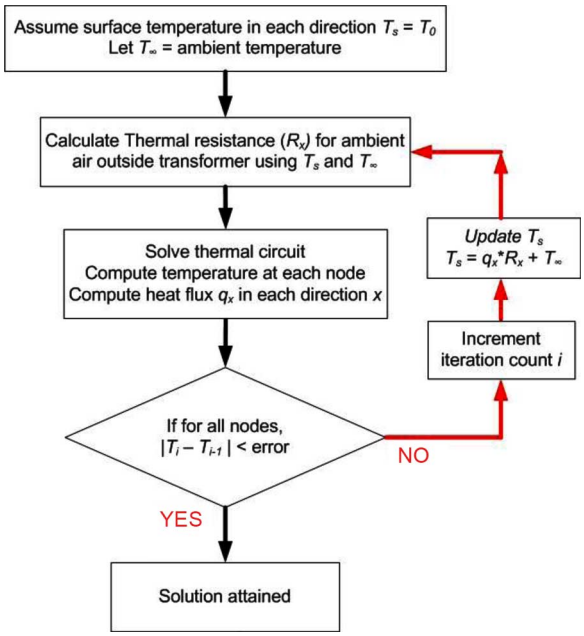


Fig. 12. Algorithm to compute temperature distribution in a transformer.

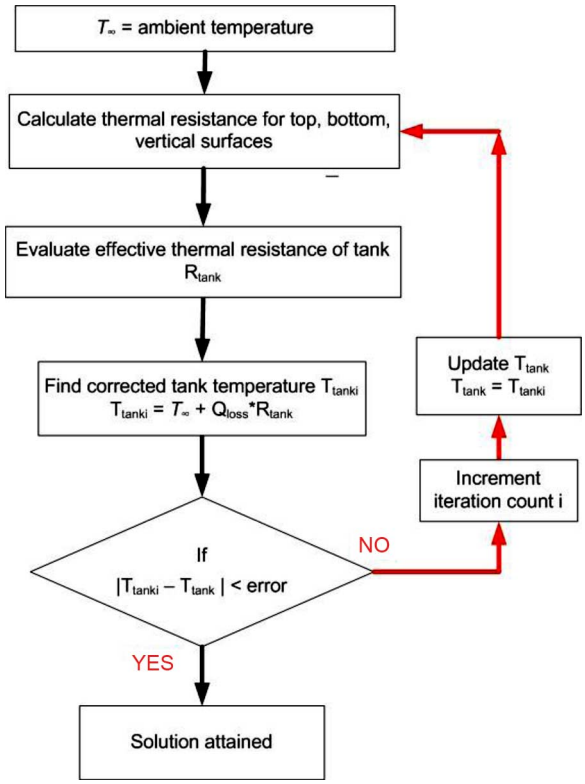


Fig. 13. Algorithm to compute the temperature of the transformer tank.

new model takes into account all geometric and electric parameters, such as physical dimensions, insulation thickness, number of turns, number of layers, and conductor gauge. The model accurately predicts the hot spots, and the knowledge is essential for the transformer designer. The model has been validated against transient FEM simulations and measurements on actual transformers. The model proposed in this paper is suitable for a toroidal transformer design computer program.

## Appendix A
## Prototype Transformer Details

120/120-V, 4 kVA, rated current 33.33 A;
core ID: 12.7 cm;
core OD: 22.86 cm;
core height: 7.62 cm;
number of layers in primary and secondary: 2 each;
turn distribution for each layer: $[118, 46, 105, 59]$;
conductor gauge: AWG 9;
insulation (Mylar) thermal conductivity $(k)$: 0.2 [W/(m. K)];
rated core loss: 14.9 (W);
full-load primary winding loss: 40.8 (W);
full-load secondary winding loss: 48.9 (W).

## Appendix B

The algorithm to compute temperature distribution within transformer is given in Fig. 12

## Appendix C

The algorithm to compute $T_{\text{tank}}$ is given in Fig. 13.

## Acknowledgment

The authors would like to thank I. Hernández and N. Augustine for their contributions and continuous support of the research work. They would also like to thank C. Prabhu for conducting all of the tests and providing results presented in this paper. Finally, the authors would like to thank U. Poulsen of Bridgeport Magnetics for his fast response and expertise in building the prototypes.

## References

[1] F. A. Furfari and J. W. Coltman, "The transformer," *IEEE Ind. Appl. Mag.*, vol. 8, no. 1, pp. 11–12, Jan./Feb. 2002.
[2] Wm. Colonel and T. McLyman, *Transformer and Inductor Design Handbook*, 3rd ed. New York: Marcel Dekker, 2004.
[3] M. van der Veen, *Modern High-end Valve Amplifiers: Based on Toroidal Output Transformers*. Maastricht, The Netherlands: Elektor Electronics, 1999.
[4] G. Swift, T. S. Molinski, and W. Lehn, "A fundamental approach to transformer thermal modeling–Part I: theory and equivalent circuit," *IEEE Trans. Power Del.*, vol. 16, no. 2, pp. 171–175, Apr. 2001.
[5] O. A. Amoda, D. J. Tylavsky, G. A. McCulla, and W. A. Knuth, "A new model for predicting hottest-spot temperatures in transformers," in *Proc. 40th North Amer. Power Symp.*, 2008, pp. 1–8.
[6] D. Susa, M. Lehtonen, and H. Nordman, "Dynamic thermal modeling of power transformers," *IEEE Trans. Power Del.*, vol. 20, no. 1, pp. 197–204, Jan. 2005.
[7] S. A. Ryder, "A simple method for calculating winding temperature gradient in power transformers," *IEEE Trans. Power Del.*, vol. 17, no. 4, pp. 977–982, Oct. 2002.
[8] A. Plesca, "3D modelling and simulation of toroidal transformers," in *Proc. 16th IASTED Int. Conf.*, 2007, pp. 358–363.
[9] I. Hernández, F. de León, and P. Gómez, "Design formulas for the leakage inductance of toroidal distribution transformers," *IEEE Trans. Power Del..*, vol. 26, no. 4, pp. 2197–2204, Oct. 2011.
[10] P. Gómez, F. de León, and I. Hernández, "Impulse response analysis of toroidal core distribution transformers for dielectric design," *IEEE Trans. Power Del.*, vol. 26, no. 2, pp. 1231–1238, Apr. 2011.
[11] *"Comsol Multiphysics, Heat Transfer Module User's Guide,"* Comsol AB Group, 2006, pp. 1–222.
[12] *IEEE Standard Test Code for Dry-Type Distribution and Power Transformers*, IEEE Standard C57.12.91-1995, Jun. 1995.
[13] O. G. Martynenko and P. P. Khramtsov, *Free Convective Heat Transfer*. Berlin, Germany: Springer-Verlag, 2005.

[14] R. B. Bird, W. E. Stewart, and E. N. Lightfoot, *Transport Phenomena*, 2nd ed. Hoboken, NJ: Wiley, 2007.
[15] S. Kakac and Y. Yener, *Convective Heat Transfer*, 2nd ed. Boca Raton, FL: CRC, 1995.
[16] M. N. Ozisik, *Heat Conduction*, 2nd ed. Hoboken, NJ: Wiley, 1993.

**Sujit Purushothaman** (S'09) received the B.Eng. degree in electrical engineering from Mumbai University (Sardar Patel College of Engineering), Mumbai, India, in 2005, and the M.Sc. and Ph.D. degrees in electrical engineering from the Polytechnic Institute of New York University, Brooklyn, NY, in 2009 and 2012, respectively.

His work experience includes testing and the development of medium-voltage switchgear for Siemens India at Kalwa Works, Mumbai. His research interests include power system transients, subsynchronous resonance damping, machine design, as well as electromagnetic modeling and thermal modeling of electrical machines.

**Francisco de León** (S'86-M'92-SM'02) received the B.Sc. and the M.Sc. (Hons.) degrees in electrical engineering from the National Polytechnic Institute, Mexico City, Mexico, in 1983 and 1986, respectively, and the Ph.D. degree from the University of Toronto, Toronto, ON, Canada, in 1992.

He has held several academic positions in Mexico and has worked for the Canadian electric industry. Currently, he is an Associate Professor at the Polytechnic Institute of New York University, Brooklyn, NY. His research interests include the analysis of power definitions under nonsinusoidal conditions, the transient and steady-state analyses of power systems, the thermal rating of cables and transformers, and the calculation of electromagnetic fields applied to machine design and modeling.